Biofuel-based Poligeneration Energy System for Electricity, Heat and Mobility Demands: Plant Design and Energy Streams Management

M. Minutillo
Department of Engineering
University of Naples "Parthenope", Naples, Italy
e–mail: mariagiovanna.minutillo@uniparthenope.it

A. Perna
Department of Civil and Mechanical Engineering
University of Cassino and Southern Lazio, Cassino, Italy
e–mail: perna@unicas.it

E. Jannelli
Department of Engineering
University of Naples "Parthenope", Naples, Italy
e–mail: elio.jannelli@uniparthenope.it

S. Ubertini
Department of Economics, Engineering, Society and Business Organization
University of Viterbo "La Tuscia", Viterbo, Italy
e–mail: stefano.ubertini@unitus.it

A. Sorce
Department of Mechanical, Energy, Management and Transportation Engineering
University of Genova, Genova, Italy
e–mail: alessandro.sorce@unige.it

ABSTRACT

Polygeneration systems represent a novel concept for the transition to sustainable low-carbon future energy systems. The plants based on this concept can use multiple energy sources (renewable and non-renewable) providing multiple energy services (heating, cooling, electricity) and other products such as fuels or water. In this way, a substantial increase in overall efficiency is achieved, and thus, indirectly, a reduction of pollution and greenhouse gas emissions.

In this paper the design of a biomass-based polygeneration system generating electricity heat and hydrogen for small refilling stations is proposed. The polygeneration system is fed by biogas, obtained from an anaerobic digester where the biomass conversion is made. It consists of i) a biogas processing unit, based on autothermal reforming technology, in which a hydrogen-rich gas is generated, ii) a power unit based on SOFC technology, iii) a hydrogen separation unit based on membrane technology and iv) a hydrogen compression and storage unit based on ionic compressor technology. The analysis has been carried out by using a numerical approach.

The system behavior has been investigated by varying the SOFC electric load from 100% to 30% (the minimum load that permits to sustain the electric power consumption of the hydrogen separation and compression units). The calculated system performance in terms of overall efficiency range from 67.5% (60% SOFC load) to 71.4% (30% SOFC load). The energy saving with respect to the separate production of electricity, heat and hydrogen ranges from 6% to 26%.

KEYWORDS: Polygeneration, Biogas, Hydrogen, SOFC, Modeling, Reforming

NOMENCLATURE

ASR	Area Specific Resistance □□ cm^2)
ATR	Autothermal Reforming Reactor
C	Compressor
CB	Catalytic burner
CCHP	Combined cooling, heating and electric power
CHP	Combined heat and power
DP	Design Point
f_{stack}	stack loss factor
j_{cell}	Cell Current density (A/cm^2)
G^t,	Total Gibbs Free Energy (J)
GHG	Greenhouse Gas
HE	Heat Exchanger
HRF	Hydrogen recovery factor
IC	Ionic compressor
L	Lagrangian function
LHV	Low Heating Value (MJ/kg)
MES	multi- energy systems
O/C	Oxidant to carbon ratio
OCV	Open Circuit Voltage (V)
Pd-M	Palladium Membrane
POX	Partial oxidation
Q	Thermal power (kW)
S/C	Steam to carbon ratio
SEP	Separation unit
SR	Steam reforming
V_{stack}	Stack Voltage (V)
V_{nom}	Nominal cell voltage (V)
W	Electric power (kW)
WGSR	Water Gas Shift Reactor
Φ□□	Chemical power of the product hydrogen (kW)
Φ_{Biogas}	Chemical power of the biogas (kW)
η_{CFP}	Overall efficiency in the co-production of fuel and power (%)
η_{el}	Electrical efficiency (%)
η_{th}	Thermal efficiency (%)
η_{H2}	Hydrogen production efficiency (%)
$\eta_{el,ref}$	Electrical efficiency of a reference technology (%)
$\eta_{th,ref}$	Thermal efficiency of a reference technology (%)
$\eta_{H2,ref}$	Hydrogen production efficiency of a reference technology (%)

BACKGROUND AND SCOPE

To meet the growing world energy demand with low GHG emission, the development of sustainable energy systems characterized by high conversion efficiency and high share of renewable in the energy mix is crucial. One of the most effective measures for increasing energy efficiency is the application of the polygeneration concept as a possible sustainable energy solution. Energy systems based on this concept can use multiple energy sources (renewable and non-renewable), providing multiple energy services (heating, cooling, electricity) and other products (water, hydrogen, etc.) [1-3]. In this way, a substantial increase in overall efficiency is achieved, and thus, indirectly, a reduction of pollution and greenhouse gas emissions.

Polygeneration technologies can be classified from different perspectives. In terms of output of energy forms, combined heat and electric power (CHP) and combined cooling, heating and electric power (CCHP) can be defined. Other useful energy forms or products can be also generated by properly combining energy inputs and devices as in the bio-refinery that can be treated as a kind of polygeneration technology. Biorefineries are similar to conventional refineries in that they produce a range of products to optimize both the use of the feedstock and production economics. Such facilities combine several fundamental process steps, including the appropriate pre-treatment, conversion and downstream processes. One challenge has always been the efficient integration of all process steps. Biorefineries converting feedstock into chemicals and materials will become the backbone of the future production of sustainable products. Small scale polygeneration systems involve a combination of conventional and new technologies for heating, cooling and electricity production, but also for other products generation such as CO2 or bio-fuels (biogas, methanol and SNG) [4-6].

In this framework this study is placed because aims to combine the development of energy systems based on high efficiency technologies like the SOFC with the co-production of electricity, heat and hydrogen by using biomass as primary source. The concept of the system is depicted in figure 1.

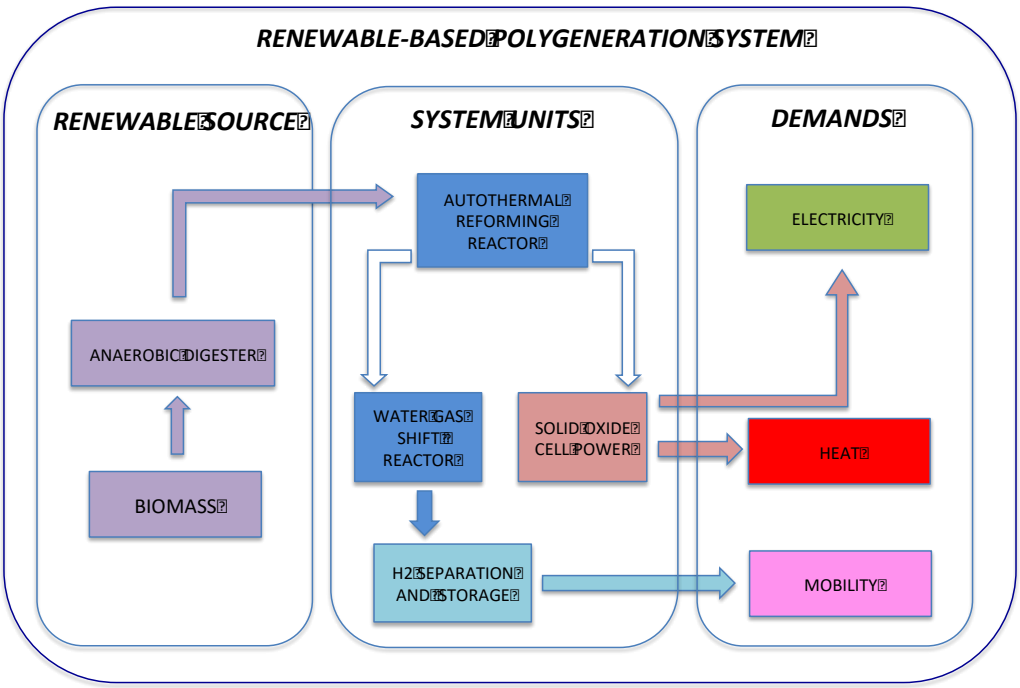

Figure 1. Conceptual scheme of the Biofuel-based polygeneration energy system

Thus, in this paper, the design of a biomass-based polygeneration system is presented and the performance analysis is carried out by applying a numerical methodology based on the development of thermo-electrochemical models.
The polygeneration system is fed by biogas, obtained from an anaerobic digester where the biomass conversion is made. It consists of i) a biogas processing unit, based on autothermal reforming technology, in which a hydrogen-rich gas is generated, ii) a power unit based on SOFC technology, iii) a hydrogen separation unit based on membrane technology and iv) a hydrogen compression and storage unit based on ionic compressor technology.
The relevance of this study is due to the analysis of a novel and advanced multi-vector energy system whose behavior is relatively unexplored, as confirmed by the limited number of published papers regarding this topic.

Polygeneration systems

Polygeneration systems represent a novel concept for the transition to sustainable low-carbon and zero-carbon future energy systems that interconnect power, transportation sectors and thermal energy demand all together [7-9].
Usually, energy sectors are de-coupled from both operational and planning viewpoints, whereas tight interactions have always taken place and are increasing. For instance, electricity, heat/cooling and fuels are produced together in the same system as a CHP system and CCHP system [10-12].
Thus, a key aspect to evolve towards a cleaner and affordable energy system is to develop integrated or multi- energy systems (MES), whereby electricity, heat, cooling, fuels, transport, and so on optimally interact with each other at various levels (for instance, within a district, or a city, or at a country level) [12].
Polygeneration systems can feature better technical, economic and environmental performance with respect to separate energy systems.
In order to be truly “poly/multi-energy” from a physical point of view, multiple energy vectors and sectors have to at different levels, from demand to generation. Hence, for the purposes of this work the concept of “multi-energy” rather refers to considering a whole-system approach to optimization and evaluation of the specific case under study (for instance, a building or a country).

Biofuels generation

The biofuels generation from biomass plays a strategic role in order to keep climate change below 2 °C as established by the European Council and Parliament that have set the long-term objective of reducing Greenhouse Gas (GHG) emissions in the European Union (EU) by 80–95% by 2050, compared to 1990 levels. Moreover, in the European Communication “Clean Power for Transport: A European alternative fuels strategy”, the wide diversification of sources for the different alternative fuels, in particular through the use of the universal energy carriers of electricity and hydrogen, biofuels, natural gas, LGP warrant security of energy supply to transport instead of oil.
Currently, biofuels contribute only in a small part to the energetic requirements in the transportation sector, so that the development of sustainable supply chains for biofuels generation and usage is one of the priority for several countries. Several biofuels supply chains, such as the bio-methane chain (both gaseous and liquid), the bio-hydrogen chain, the methanol chain, the butanol chain and other liquid biofuels chains for transport and chemical industry applications, are considered of strategic interest for a sustainable development.
Hydrogen gas (H_2) is a valuable energy carrier, an important feedstock to the chemical industry, and useful in detoxifying a wide range of water pollutants. As an energy carrier, it is especially attractive due to its potential to be used to power chemical fuel cells. Often

hydrogen is converted into Hydro-methane (a blend of methane and hydrogen, where H_2 maximum volume content is 30%), which is easier to be stored and transported to the refueling stations, considering its higher energy content in volume terms [13].

BIOFUEL-BASED POLYGENERATION ENERGY SYSTEM DESCRIPTION

This study is focused on the design of a polygeneration system fed by biogas generated from the biomass anaerobic digester. In the system, by means of hydrogen-based technologies like autothermal reforming and SOFC, it is possible to satisfy electricity, heat and mobility demands by starting form biomass conversion in anaerobic digester. Figure 2 shows the plant scheme.

Biogas, air and water are heated in the heat exchangers HE2 (300°C), HE3 (580°C) and HE4 (580°C), respectively, before entering in the ATR reactor (autothermal reforming reactor). The produced syngas (6), that leaves the ATR at 771°C, is cooled at 320°C (HE7) and then is separated in two fluxes: the stream (7) is sent to the WGSR (water gas shift reactor) and the stream (AN-IN) is used for feeding the SOFC (solid oxide fuel cell) unit. The heat from the WGSR effluent is recovered in the heat exchanger HE8, so that the stream is dried before to be compressed (compressor C) to 11 bar and heated (HE5) to reach the operating conditions of the the membrane unit (Pd-M), where hydrogen is separated. Thus, the pure hydrogen (12) is cooled (HE9) and compressed (IC) at 820 bar according to the requirements of a hydrogen refilling station, while the purge gas (13) is combusted (CB) with the cathode off-gas (CATH-OFF), the anode off-gas (AN-OFF) and the fresh air (2). The combustor effluent exchanges heat with more streams (heat exchangers HE3, HE4, HE5, HE6), before being exhausted (22) at 105 °C. The air for the cathode (1) is pre-heated before entering the cathode (CATH-IN) at about 400 °C. The heat exchangers devoted to the thermal demand are HE6, HE7, HE8 and HE9.

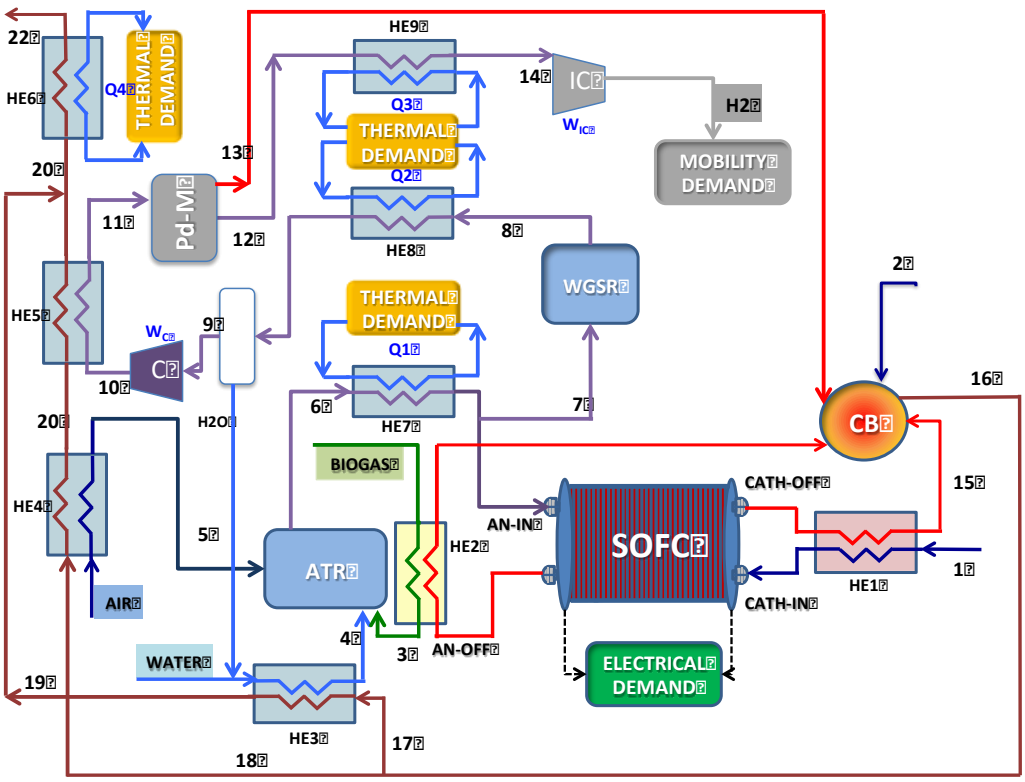

Figure 2. Lay-out of the polygeneration system

METHODOLOGY

The employed methodology is based on a numerical approach that consists in the implementation and integration of the thermochemical and electrochemical submodels developed for each unit and component. Figure 3 shows the flowsheet of the integrated model, realized by using the Aspen One code. In this study, the energy and mass balances of the bio-chemical conversion of the biomass into biogas (60% CH_4, 40% CO_2) via anaerobic digestion is not considered.

The model integrates the system units, simulated by means of five Hierarchy blocks whose inlet and outlet streams are labeled according with those defined in figure 2. They are:

-BPUNIT: it consists of an autothermal reactor and a water gas shift reactor, simulated by means of chemical equilibrium reactor blocks *RGibbs*;

-SOFC: the anode is simulated by a stoichiometric reactor block *RStoich* in which the electro-oxidation reaction takes place and a *RGibbs* reactor block in which the reforming reaction and/or the water gas shift reaction that can occur during the fuel cell operation are considered. The cathode side is modeled by a *Separator* block in which the oxygen is separated from the incoming cathode flow and sent to the anode side according to the assigned utilization factor. Moreover, a heat exchanger to simulate the preheating of the cathode air is also considered.

-MSUNIT: it consists of a compressor to reach the membrane operating pressure and a Fortran block calculator where the membrane model, that will be explained later, is implemented.

-ICUNIT: it consists of a *Multistage Compressor* block;

-THUNIT: in this hierarchy block the thermal balance of the plant according with the thermal fluxes and heat exchanges shown in figure 2 is modeled. Therefore, it consists of seven heat exchangers and a catalytic burner simulated by means of a stoichiometric reactor block *RStoich*.

A detailed description of the working conditions and behavior of each unit is presented in the following.

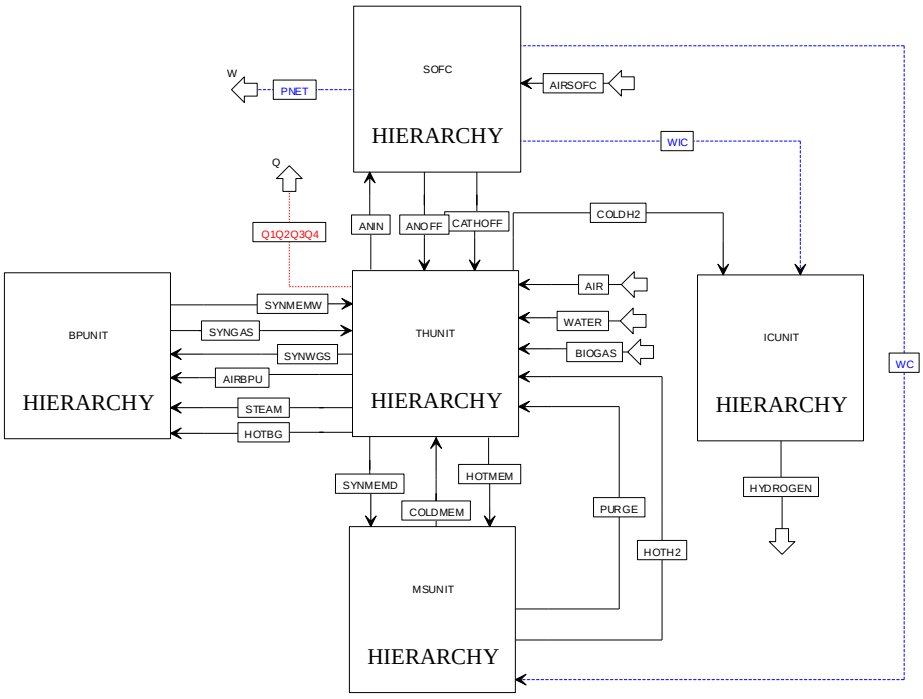

Figure 3. Flowsheet of the polygeneration system model

Autothermal Reforming process

The autothermal reforming (ATR) combines the partial oxidation reforming and the steam reforming in a single process in which the oxidation of a portion of reactants supplies the energy required for the endothermic reforming reaction whereas the reforming controls temperature excursions of the oxidation reactions, so that the reactor is globally in thermally self-sustaining condition. Thus, the operating parameters of the process are the steam to carbon ratio (S/C), the oxidant to carbon ratio (O/C) and the reforming temperature [14]. In order to maximize the hydrogen production, the process is carried out in two steps: i) high-temperature step (the main reactions are the partial oxidation and the steam reforming), in which the fuel is converted into a gaseous mixture of H_2, CO, CO_2, N_2, and H_2O; ii) low temperature step (the main reaction is the water gas shift), in which CO is reacted with H_2O towards H_2 and CO_2. As a result, the fuel processor unit consists of an ATR reactor and a WGSR reactor.

Due to the operating temperature of the shifter (about 200-400°C), the syngas coming from the ATR must be cooled before entering the WGSR.

Due to the complexity of the reaction system, the thermodynamic equilibrium analysis is determined by the non-stoichiometric approach. In this approach the equilibrium composition of the system is found by the direct minimization of the Gibbs free energy for a given set of species without any specification of the possible reactions which might take place in the system.

The species considered are: H_2, CO, CO_2, H_2O, N_2, O_2, CH_4, C(s).

The total Gibbs free energy of a system, G^t, is defined as:

$$G^t = \sum_{i=1}^{N} n_i \cdot \mu_i \qquad (1)$$

where n_i is the number of moles of species i, and μ_i is the chemical potential of species i. The problem is to find the values of n_i which minimize the objective function G^t. The appropriate method, which is usually performed for the minimization of the Gibbs free energy problem, is the Lagrange multipliers. The constraint of this problem is the elemental balance, i.e.

$$\sum_{i=1}^{N} n_i \cdot a_{i,j} = A_j \qquad j=1, 2,\ldots,k \qquad (2)$$

where $a_{i,j}$ is the number of atoms of the jth element in a mole of the ith species. A_j is defined as the total number of atoms of the jth element in the reaction mixture. To form the Lagrangian function (L), the Lagrange multipliers, $\lambda_j = \lambda_1, \ldots, \lambda_k$, are used by multiplying with elemental balance constraints, and those terms are subtracted from G^t, as follows:

$$L = G^t - \sum_{j=1}^{k} \lambda_j \left(\sum_{i=1}^{N} n_i \cdot a_{i,j} - A_j \right) \qquad (3)$$

The partial derivatives of Eq. (3) are set equal to zero in order to find the extremum point:

$$\frac{\partial L}{\partial n_i} = 0 \qquad (4)$$

Eq. (4) can be formed in terms of a matrix that has i rows, and those are solved simultaneously with the constraints as defined in Eq. (2) and the solutions n_i must be real numbers in the boundary $0 < n_i < n_{tot}$. Eq. (4) creates the set of non-linear equations solved by an iteration technique.

The equilibrium compositions have been calculated for a given operating condition and, in order to evaluate the overall efficiency, the material and energy balances are solved for each

configuration. The results obtained by the thermochemical models are in accordance with scientific literature confirming the effectiveness of chemical equilibrium to predict the syngas composition in the catalytic reforming processes.

SOFC power unit

The electrochemical model of the SOFC unit is based on the single cell numerical model detailed in [15] and further improved in [16]. In this single cell model, the cell is discretized in N-elements along both the anodic and cathodic flow directions and each J-element consists of anode, cathode and electrolyte. In order to predict the cell behavior and performances under different operating conditions (pressure, temperature, flows composition, anode and cathode utilization factors), mass and energy balances are calculated by taking into account both the electrochemical (i.e. electro-oxidation of hydrogen and electro-reduction of oxygen) and the thermochemical reactions (i.e. reforming and shifting reactions) that can occur in the anode side and cathode side, as widely explained in [15,16].
The up-scaling from small single cell to stack level leads to a drop-in performance, because the homogeneity in electrical contact and gas distribution is more difficult to achieve. Thus, the single cell model has been adjusted to predict the behavior and performances at stack level by means of the area-specific resistance (ASR, Ωcm^2) usually employed to quantify the losses associated with the fuel cell operations. This cell performance parameter is often defined as the slope of the chord between the OCV and the design operating point (DP) in the voltage-current density plane (V,j):

$$ASR = \frac{|OCV - V_{DP}|}{j_{DP}} \tag{5}$$

Therefore, in accordance with the analysis carried out in [17], a stack loss factor has been defined as:

$$f_{stack} = \frac{ASR_{stack}}{ASR_{cell}} \tag{6}$$

Therefore, the stack voltage is calculated as:

$$V_{stack} = ASR_{stack} j_{cell} n_{cell} \tag{7}$$

where n_{cell} is the cells number in the stack.
All details on the SOFC model, like equations and calibration parameters, are illustrated in ref. [16,17].

Membrane separation unit

The membrane separation unit, based on Palladium (Pd) and its alloys, is formed by multi-tube membrane modules. Each module consists of a bundle of permeator tubes where the gas mixture is fed in the tube lumen and the separated hydrogen is collected in the shell side while the retentate leaves the membrane lumen [18].
The permeation of hydrogen through a metallic (such as Pd) film is a complex process that involves sorption of hydrogen molecules on the film surface and desorption from the ceramic substrate [19]. The hydrogen molecule dissociates into hydrogen atoms on the high-pressure side (feed side) of the film, then diffuses through the film and re-associate on the low-pressure side (permeate side).
The hydrogen permeation flux is:

$$J_{H_2,perm} = \frac{Pe}{s} \cdot \Delta P \tag{8}$$

where Pe (m^3 m^{-1} s^{-1} $Pa^{-0.5}$) is the hydrogen permeability, s (m) is the membrane tube thickness and ΔP (Pa^5) is the driving force of permeation.
The hydrogen permeability, Pe, can be calculated following an Arrhenius type law:

$$Pe = Pe_0 \cdot e^{\frac{-E_a}{RT}} \tag{9}$$

where Pe_0 (m^3 $m^{-1}s^{-1}Pa^{-0.5}$) is the pre-exponential factor, E_a (J mol^{-1}) is the activation energy for permeation (equal to the sum of the diffusion energy and the heat of dissolution), R (J mol^{-1} K^{-1}) is the gas constant, e T (K) is the operating temperature.
Since the dissociation reaction kinetics of hydrogen and the reverse reaction are relatively fast, the diffusion of hydrogen atoms through the metal film is generally the rate-limiting step, so that the hydrogen flux through the selective membrane can be described by the Sievert's law [19].
The permeation driving force can be expressed by the log mean difference of the partial pressure square roots calculated at the inlet and outlet of the permeator tube [18]:

$$\Delta P_{LMDP} = \frac{\left(p_{H_2,feed}^{0.5} - p_{H_2,perm}^{0.5}\right)_{in} - \left(p_{H_2,feed}^{0.5} - p_{H_2,perm}^{0.5}\right)_{out}}{ln\frac{\left(p_{H_2,feed}^{0.5} - p_{H_2,perm}^{0.5}\right)_{in}}{\left(p_{H_2,feed}^{0.5} - p_{H_2,perm}^{0.5}\right)_{out}}} \tag{10}$$

where $p_{H2,feed}$ (Pa) is the hydrogen partial pressure at the feed side of the membrane, $p_{H2,perm}$ (Pa) is the hydrogen partial pressure at the permeate side.
The efficiency of the permeation process is estimated by means of the hydrogen recovery factor (HRF), defined as the ratio between the flow rate of the H_2 permeated through the membrane and the H_2 feed flow rate:

$$HRF = \frac{n_{H_2,perm}}{n_{H_2,feed}} \tag{11}$$

The hydrogen permeation flow rate (mol s^{-1}) is given by:

$$n_{H_2,perm} = J_{H_2,perm} \cdot A_{perm} \tag{12}$$

where A_{perm} (m^2) is the permeation area that is obtained by combining Eqs 8,11,12.
In a multi-tubes configuration the membrane permeation area can be expressed by considering the single tube permeation area ($\pi D L$) and the number of tubes (N_t):

$$A_{perm} = N_t \cdot \pi \cdot D \cdot L \tag{13}$$

where D (m) and L (m) are the diameter and the length of the tube, respectively.
The choice of the geometric parameters (s,D,L) depends on the mechanical strength of the tube (it have to increase as the driving force increases) and on the tensile strength of the Pd-Ag alloy that decreases when the operating temperature rises.
Therefore, in order to minimize the permeation area the sizing of the membrane separation unit is carried out by an iterative procedure in which the designing parameters are the hydrogen recovery ratio HRF, the feed and the permeate sides pressures and the membrane operating temperature that will be chosen by taking into account the constrain on the mechanical strength of the tube.
The model of the membrane separation unit has been implemented in Fortran language in the MS (Membrane Separation) sub-model.

High pressure hydrogen storage

In the hydrogen compression and storage section the hydrogen is compressed until to the pressure (820 bar) of the storage tanks. The technology selected for the hydrogen compression is based on the liquid ionic compressors developed by Linde [20-22]. Ionic compressors are

similar to conventional reciprocating compressors but use nearly incompressible ionic liquids in place of the metal piston. Thus, the gas is compressed in the cylinder by the up-and-down motion of the liquid column, similar to the reciprocating motion of an ordinary piston [20]. These compressors do not require bearings and seals, two of the common sources of failure in reciprocating compressors and are characterized by high-performance.
The working operating conditions (pressure ratio) and configuration (number of stages) of this compressor are like those of the ionic compressor IC-90 developed by Linde Group [20]. In particular, as reported in [21], in order to reach the storage pressure, the IC-90 consists of 5 stages operating with a pressure ratio of 2.8. The specific energy consumption is equal to 2.7 kWh/kg_{H2} and the energy saving in comparison with conventional reciprocating compressors is around 40%. Moreover, the liquid acts as a medium to carry heat out of the compression chamber, allowing near-isothermal operation [23].
Therefore, the ionic compressor (IC) has been modeled by considering five compression stages formed by an adiabatic compressor and a heat exchanger. The polytropic efficiency of each adiabatic compressor is chosen by taking into account the specific work consumption of the IC-90, whereas in order to achieve near-isothermal conditions the removed thermal power in each heat exchanger is assumed equal to the 90% of the corresponding adiabatic compressor power consumption.

Thermal Unit

The thermal management of the system is performed by using several heat exchangers that are used both to heat/cool the streams according to the required/assigned temperatures and to produce heat for the utility. The heat exchangers HE6, HE7, HE8 and HE9 are devoted to produce hot water for thermal demands; for these components the thermal efficiency has been assumed equal to 0.85. The thermal efficiency of the gas/gas heat exchangers (HE1, HE2, HE4, HE5) has been assumed equal to 0.75.
In order to account for the off-design conditions, the thermal efficiencies of all the heat exchangers vary from their maximum values (0.85 or 0.75) to a minimum value (about 0.65).

RESULTS AND DISCUSSION

In order to define the SOFC power unit configuration in terms of modules number, stacks number and cells number per stack, the single cell polarization curve is calculated by considering the cell characteristics reported in [16]. Then, the cell-stack voltage has been estimated by applying Eqs. (6,7) in the operating voltage range OCV-V_{nom}. As stack operating conditions, the current density and the fuel utilization factor are chosen equal to 0.5 A/cm^2 and 0.8, respectively. Moreover, in order to simplify the stack thermal management, the stack cooling is performed by the anode and cathode flow rate (the air utilization factor is kept in accordance with the working conditions of the single SOFC described in [16], so that the optimal stack temperature is 800°C: the cell operating voltage results equal to 0.75 V. By fixing the cell area (500 cm^2), the SOFC power unit, sized for the maximum syngas flow rate coming from the BP unit, consists of five modules (each module is formed by 4 stacks with 55 cells per stack). This configuration allows to manage the power unit almost at nominal stack power also at partial loads.
The sizing of the membrane separation unit has been based on the minimization of the permeation area for the specified *HRF* and, from a system level point of view, on the minimization of the power consumption to reach the membrane operating pressure.
Therefore, by fixing the permeate side pressure equal to 1.1 bar, the feed side pressure of 11 bar has been chosen by considering both its positive effect on the permeation (higher

pressures lead to higher driving forces) and its negative impact on the mechanical stress of the tubes (higher pressures require higher tube thicknesses) as well as on the system energy balance (a greater compression power is required to achieve the membrane operating pressure). Moreover, the geometry of the single tube (tube diameter, thickness and length) has been selected by considering both the desired mechanical performance and the commercial availability, as suggested in [18]. For commercial permeator tubes, the diameter can vary between 10 and 25 mm, the wall thickness is in the range 0.050-0.200 mm, while the length of the tube may reach the meter. Thus, by keeping s=0.14 mm, D=12 mm and L=0.6 m, in the maximum hydrogen production (electric load 30%) the membrane separation unit is made of 14 modules with 124 tubes per module.

The ionic compressor has been modeled by considering the specific power consumption of the IC-90 manufactured by Linde. Thus, in order to have this specific power consumption the polytropic efficiency of each adiabatic stage has been set to 0.91, whereas in order to reach a near-isothermal conditions the thermal power removed in each stage has been set to 90% of that generated during the compression stage.

The system behavior has been investigated by varying the SOFC electric load from 100% to 30%. This minimum load has been set because it permits to sustain the electric power consumption of the hydrogen separation and compression units). Thus, eight operation cases have been analyzed.

The system efficiencies have been calculated as follows.

The electrical efficiency is:

$$\eta_{el} = \frac{W}{\Phi_{Biogas}} \tag{14}$$

The thermal efficiency is:

$$\eta_{th} = \frac{Q}{\Phi_{Biogas}} \tag{15}$$

The hydrogen production efficiency, referred to the low heating value (LHV) is:

$$\eta_{H2} = \frac{\Phi_{H2}}{\Phi_{Biogas}} \tag{16}$$

Thus, the overall efficiency in the co-production of fuel and power (electric and thermal) is [20]:

$$\eta_{CFP} = \frac{W + Q + \Phi_{H2}}{\Phi_{Biogas}} \tag{17}$$

In Eqs. (14) – (17), W is the net electric power, Q is the available thermal power, Φ_{H2} is chemical power of the product hydrogen (LHV is 120 MJ/kg) and Φ_{Biogas} is the chemical power of the biogas feeding the polygeneration system (LHV is 17.7 MJ/kg).

Furthermore, in order to evaluate the energy saving obtained by the polygeneration of electricity, heat and hydrogen with respect to their separate production in reference technologies, the energy saving factor (ES) has been introduced as further performance parameter:

$$ES = 1 - \frac{1}{\frac{\eta_{el}}{\eta_{el,ref}} + \frac{\eta_{th}}{\eta_{th,ref}} + \frac{\eta_{H2}}{\eta_{H2,ref}}} \tag{18}$$

where the electric, thermal and hydrogen reference efficiencies result to be equal to 42%, 75% and 64%, respectively. The reference electric and thermal efficiencies are the values suggested in [24] and referred to biogas-based plants, whereas the reference hydrogen efficiency is calculated by taking into account the energy consumption of alkaline electrolyzer technology (4.4 kWh/Nm^3_{H2}[25]) and the energy consumption for hydrogen compression and storage (2.7 kWh/kg_{H2} by applying the ionic compressor technology [21]).
The system behavior has been investigated by varying the SOFC electric load from 100% to 30% (the minimum load that permits to sustain the electric power consumption of the hydrogen separation and compression units). Thus, eight operation cases have been analyzed.
Modeling results, in terms of stream thermodynamic conditions, chemical, electrical and thermal powers are illustrated in tables 1 and 2.

Table 1. Streams characteristics at different SOFC loads

	SOFC LOAD (%)			
	30		100	
Streams	Mass flows (kg/h)	Temperature (°C)	Mass flows (kg/h)	Temperature (°C)
BIOGAS	104.5	20	104.5	20
AIR	189.2	20	189.2	20
WATER	83.6	20	83.6	20
AN-IN	113.2	320	377.4	320
CATH-IN	185.4	400	617.9	400
AN-OFF	137.5	800	458.1	00
CATH-OFF	160.9	800	536.3	800
H2	6.2	69	-	-
1	185.4	20	617.9	20
2	144.2	20	144.2	20
3	104.5	300	104.5	300
4	83.6	580	83.6	580
5	189.2	580	189.2	580
6	377.4	771	377.4	771
7	264.2	320	-	-
8	264.2	399	-	-
9	229.7	20	-	-
10	229.8	175	-	-
11	229.8	400	-	-
12	6.2	400	-	-
13	223.6	400	-	-
14	6.2	20	-	-
15	160.9	257.4	536.3	254
16	666.2	883	1138.7	697
17	399.7	883	683.2	697
18	266.5	883	455.5	697
19	399.7	126	683.2	262
20	266.5	453	455.5	446
21	666.2	118	1138.7	336
22	666.2	105	1138.7	105

As reported in table 1, 100% means that the biogas is totally used for SOFC feeding, so that the section of the system regarding the compressed hydrogen production does not work. On the contrary, at the partial load of 30%, the system produces the maximum hydrogen flow rate.
Table 2 summarizes the thermal, electrical and chemical powers for the 8 cases. It can be noted that the net electric power ranges from 10 to 204 kW. The electric power at SOFC load equal to 30% (10kW) has been chosen as the minimum value that has to be guaranteed to satisfy the electric power consumption of the hydrogen separation and compression units. By analyzing the thermal power production, it can be noted that the highest value (154.3 kW) is reached at the SOFC full load operation. This thermal power is totally due to the exhausts from the catalytic burner (Q4 at HE6) and from the heat exchanger HE7 (Q1) that is used to cool the syngas exiting the ATR from 771°C to 320°C. This last thermal power does not change by varying the SOFC load because the heat is recovered by cooling the total syngas mass flow rate (before to be split in two streams).
In table 2 the energy saving factor (ES) is also reported. It can be noted that the polygeneration system permits to achieve an energy saving in the whole operating range. The energy saving rises with the increasing of the electric load and reaches 25.7% as the SOFC works at rated power (100% load).

Table 2. Energy balance in the operational range (Φ_{Biogas} = 513.5 kW)

		SOFC LOAD (%)							
		30	40	50	60	70	80	90	100
Thermal Power (kW)	Q_1	68.4	68.4	68.4	68.4	68.4	68.4	68.4	68.4
	Q_2	69.5	58.4	44.7	31.8	22.4	13.9	6.4	-
	Q_3	9.5	8.0	6.1	4.3	3.1	1.9	0.9	-
	Q_4	1.8	10.0	19.8	30.7	42.8	56.3	70.1	85.9
	Q	149.2	144.9	139.1	135.2	136.7	140.5	145.9	154.3
Electric Power (kW)	W_C	29.4	22.9	16.8	16.8	11.3	6.7	2.9	-
	W_{IC}	22.5	19.3	16.1	12.9	9.7	6.4	3.2	-
	W_{SOFC}	62	82	102	123	144	164	184	204
	W	10.1	39.8	69.1	93.3	123.0	150,9	177,9	204.0
Chemical Power (kW_{LHV})	Φ_{H2}	207.3	178.0	148.0	118.3	89.0	59.3	29.3	-
Energy saving factor	ES (%)	6.1	9.3	11.6	12.6	16.4	19.7	22.6	25.7

In figure 4, the hydrogen chemical power and the thermal power vs the electric power are depicted. As it is expected the hydrogen available from the system increases when less electric power is produced. Moreover, it can be observed that, the thermal power trend reaches a minimum value at 60% SOFC load (at 93.3 kW).

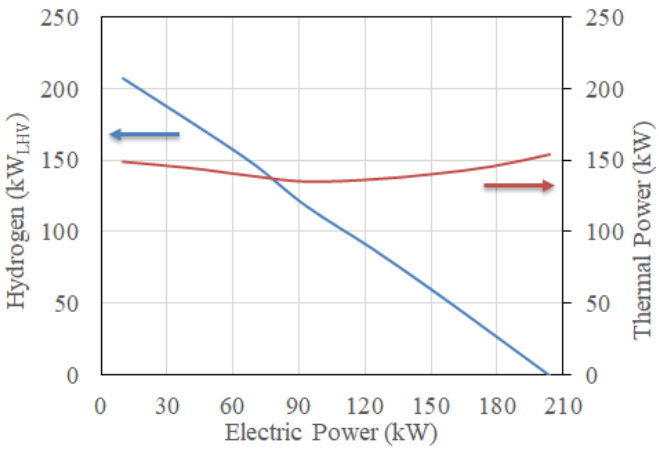

Figure 4. Performance curves

Figure 5 show the polygeneration system efficiencies vs the electric load. It is worth nothing that the overall efficiency (CFP efficiency) trend is almost constant as the electric load varies. The minimum value is 67.5 % (at 60% SOFC load) while the maximum efficiency of 71.4% is reached at the minimum SOFC load (30%); this result shows that, from the overall performance point of view, the best value is obtained when in the system the highest hydrogen production rate is produced. On the other hand, as it is expected, the electric efficiency and hydrogen production efficiency trends increases and decreases with the SOFC load, respectively. Their behaviors result to be complementary (the maximum efficiency is about 40% for both). The thermal efficiency ranges from 26.3% (60% SOFC load) to 30.1% at the maximum SOFC load.

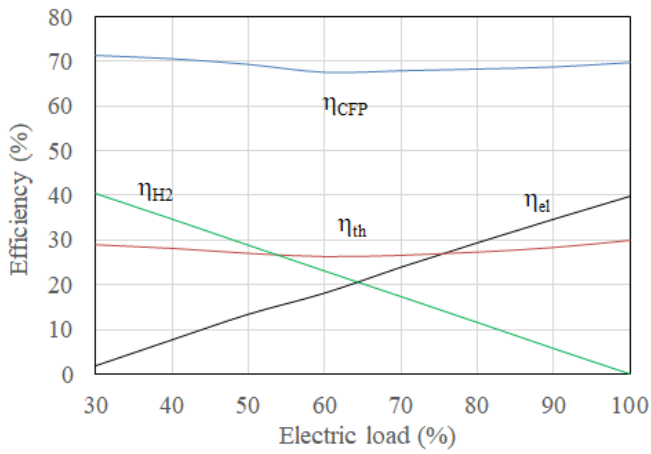

Figure 5. Polygeneration system efficiencies

CONCLUSION

In this paper, the design of a biofuel-based polygeneration system is presented and the performance analysis is carried out by applying a numerical methodology based on the development of thermo-electrochemical models.

The polygeneration system consists of a biogas autothermal reforming unit, a SOFC unit, a Pd-membrane hydrogen separation unit and a hydrogen compression and storage unit.

The system behavior has been investigated by varying the SOFC electric load from 100% to 30% (the minimum load that permits to sustain the electric power consumption of the hydrogen separation and compression units). Thus, eight operation cases have been analyzed.
The system has been designed to generate a maximum electric power of 204 kW (39.7% electric efficiency) and a maximum hydrogen flow rate of 6.2 kg/h (207.3 kW). The thermal power available for satisfying a thermal utility is in the rage 135- 154 kW.
The best performance in terms of overall efficiency (η_{CFP}) is 71.4%. This performance is reached at 30% SOFC load.
The system proposed and analyzed in this study is an advanced polygeneration system that represents an interesting multi-energy solution with an energy saving with respect to the separate production ranging from 6% to 26%.
Thus, results show that by using a renewable source and by interconnecting thermal and electric energy demands with the biofuel generation for transportation the transition to a sustainable zero-carbon future is feasible.

REFERENCES

1. Ghaem Sigarchian S, Malmquist A, Martin V. The choice of operating strategy for a complex polygeneration system: A case study for a residential building in Italy. Energy Conversion and Management 2018;163: 278-291
2. Serra LM, Lozano MA, Ramos J, Ensinas AV, Nebra SA. Polygeneration and efficient use of natural resources Energy 2009; 34:575–586
3. Calise F, Cipollina A, Dentice D'Accadia M, Piacentino A. A novel renewable polygeneration system for a small Mediterranean volcanic island for the combined production of energy and water: Dynamic simulation and economic assessment. Applied Energy 2014; 135:675–693
4. M. Minutillo, A. Perna, A Novel Approach for Treatment of CO2 from Fossil Fired Power Plants. Part B: The Energy Suitability of Integrated Tri-Reforming Power Plants (ITRPPs) for Methanol Production, Int. Journal of Hydrogen Energy,2010;35:7012-7020.
5. Minutillo M, Perna A. Renewable Energy Storage System via coal hydrogasification with co-production of electricity and synthetic natural gas, Int. Journal of Hydrogen Energy. 2014;39:5793-5803.
6. Rivarolo M., Cuneo A., Traverso A., Massardo A.F., Design optimisation of smart poly-generation energy districts through a model-based approach, Applied Thermal Engineering, 2016; 99:291-301
7. Bracco S, Delfino F, Pampararo F, Robba M, Rossi M.Dynamic optimization-based architecture for polygeneration microgrids with tri-generation, renewables, storage systems and electrical vehicles. EnergyConversion and Management 2015, 96:511–520
8. Gimelli A, Muccillo M. The Key Role of the Vector Optimization Algorithm and Robust Design Approach for the Design of Polygeneration Systems. Energies 2018;11(4):821; doi:103390/en11040821 ISSN 1996-1073
9. Calise F, Figaj RD, Massarotti N, Mauro A, Vanoli L. Polygeneration system based on PEMFC, CPVT and electrolyzer: Dynamic simulation and energetic and economic analysis. Applied Energy 2017; 192:530–542
10. Facci, A. L., Ubertini, S. Meta-heuristic optimization for a high-detail smart management of complex energy systems.Energy Conversion and Management 2018; 160:341-353.
11. Facci, A. L., Ubertini, S. Analysis of a fuel cell combined heat and power plant under realistic smart management scenarios. Applied Energy, 2018;216:60-72.
12. Mancarella P., Multi-energy systems: An overview of concepts and evaluation models, Energy 2014;65 (C):1-17

13. Bellotti D., Rivarolo M, Magistri L., Massardo A.F., Thermo-economic comparison of hydrogen and hydro-methane produced from hydroelectric energy for land transportation, International Journal of Hydrogen Energy, 2015; 40:2433-2444
14. Perna A.Theoretical analysis on the autothermal reforming process of ethanol as fuel for a proton exchange membrane fuel cell system. Journal of Fuel Cell Science and Technology 2007; 4 (4):468-473
15. Minutillo M, Perna A, Jannelli E. SOFC and MCFC system level modeling for hybrid plants performance prediction. Int. J Hydrogen, Energy 2014; 39: 21688-99
16. Perna A, Minutillo M, Jannelli E., Cigolotti V., Nam SW, Yoon KJ. Performance assessment of a hybrid SOFC/MGT cogeneration power plant fed by syngas from a biomass down-draft gasifier. Applied Energy 2017, https://doi.org/10.1016/j.apenergy.2017.08.077.
17. Perna A, Minutillo M, Jannelli E. Designing and analyzing an electric energy storage system based on reversible solid oxide cells. Energy Conversion and Management 2018;159:381-95
18. Bruni G, Cordiner S, Tosti S. A novel procedure for the preliminary design of dense metal membrane modules for hydrogen separation. International Journal of Hydrogen Energy 2016; 44(41):20198-209.
19. Perna A., Cicconardi S.P., Cozzolino R. Performance evaluation of a fuel processing system based on membrane reactors technology integrated with a PEMFC stack. International Journal of Hydrogen Energy 2011;36(16):9906-15
20. Linde. Hydrogen technologies. The Ionic Compressor 90 MPa – IC90. Technical brochure; 2015
21. Mayer M. From prototype to serial production: Manufacturing hydrogen fuelling stations. A3PS Ecomobility Conference, 20 October 2014, Vienna, Austria.
22. Linde. Linde's innovative technologies for the hydrogen infrastructure. 2015
23. Van de Ven JD, Li PY. Liquid piston gas compression. Applied Energy 2009; 86(10):2183-91
24. COMMISSION DELEGATED REGULATION (EU) 2015/2402 of 12 October 2015, https://eur-lex.europa.eu/legal-content/IT/TXT/?uri=CELEX%3A32015R2402
25. Perna A, Minutillo M, Jannelli E. Hydrogen from intermittent renewable energy sources as gasification medium in integrated waste gasification combined cycle power plants: a performance comparison. Energy 2016;94:457-465